BIOCHEMISTRY
including biophysical chemistry & molecular biology

Article

pubs.acs.org/biochemistry

Transthyretin as both a Sensor and a Scavenger of β-Amyloid Oligomers

Dennis T. Yang,[†] Gururaj Joshi,[‡] Patricia Y. Cho,[†] Jeffrey A. Johnson,[‡] and Regina M. Murphy*[,†]

[†]Department of Chemical and Biological Engineering and [‡]School of Pharmacy, University of Wisconsin, Madison, Wisconsin 53706, United States

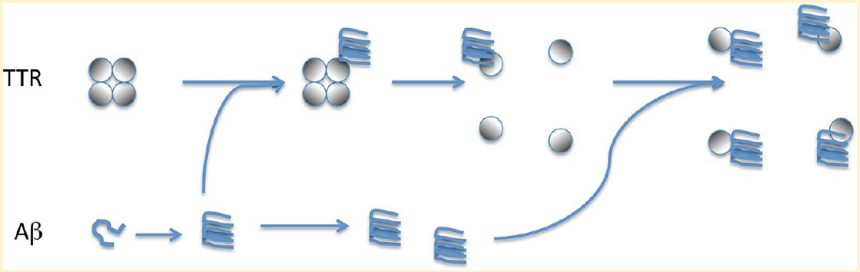

ABSTRACT: Transthyretin (TTR) is a homotetrameric transport protein, assembled from monomers that each contain two four-stranded β-sheets and a short α-helix and loop. In the tetramer, the "inner" β-sheet forms a hydrophobic pocket while the helix and loop are solvent-exposed. β-Amyloid (Aβ) aggregates bind to TTR, and the level of binding is significantly reduced in mutants L82A (on the loop) and L110A (on the inner β-sheet). Protection against Aβ toxicity was demonstrated for wild-type TTR but not L82A or L110A, providing a direct link between TTR−Aβ binding and TTR-mediated cytoprotection. Protection is afforded at substoichiometric (1:100) TTR:Aβ molar ratios, and the level of binding of Aβ to TTR is highest for partially aggregated materials and decreased for freshly prepared or heavily aggregated Aβ, suggesting that TTR binds selectively to soluble toxic Aβ aggregates. A novel technique, nanoparticle tracking, is used to show that TTR arrests Aβ aggregation by both preventing formation of new aggregates and inhibiting growth of existing aggregates. TTR tetramers are normally quite stable; tetrameric structure is necessary for the protein's transport functions, and mutations that decrease tetramer stability have been linked to TTR amyloid diseases. However, TTR monomers bind more Aβ than do tetramers, presumably because the hydrophobic inner sheet is solvent-exposed upon tetramer disassembly. Wild-type and L110A tetramers, but not L82A, were destabilized upon being co-incubated with Aβ, suggesting that binding of Aβ to L82 triggers tetramer dissociation. Taken together, these results suggest a novel mechanism of action for TTR: the EF helix/loop "senses" the presence of soluble toxic Aβ oligomers, triggering destabilization of TTR tetramers and exposure of the hydrophobic inner sheet, which then "scavenges" these toxic oligomers and prevents them from causing cell death.

An important pathological feature of Alzheimer's disease (AD) is deposition of aggregates of β-amyloid (Aβ) in extracellular plaques, primarily in the hippocampus and cerebral cortex. These amyloid deposits figure prominently in the dominant current hypothesis regarding the cause of AD, specifically, that aggregates of Aβ are toxic to neurons, by a still-undefined mechanism. Aβ is a proteolytic cleavage product of the transmembrane amyloid precursor protein (APP). Most cases of AD arise sporadically late in life; however, there are genetically linked cases of early onset AD that are linked to mutations in APP, where there is aggressive Aβ deposition. Early efforts to establish a transgenic mouse as an AD model, by engineering expression of the Swedish mutation of APP (APP_{Sw}), were not entirely successful. Although amyloid deposits were abundant, the mice did not progress to develop other characteristics of the disorder such as neurofibrillary tangles or widespread neuronal loss. As a possible explanation for the lack of AD-like pathology, Stein and Johnson observed a spontaneous 8-fold increase in the level of expression of the gene for transthyretin (TTR) in APP_{Sw} mice and showed that infusion of anti-TTR antibodies led to increased levels of tau phosphorylation and neuronal loss. These results strongly suggest that an increased level of TTR expression protects APP_{Sw} mice from AD-like pathologies.[1,2] An increased level of TTR expression in mouse models of AD has been confirmed by other groups.[3−5] Furthermore, neurons from human AD patients, but not age-matched controls, secrete TTR.[5] The protective effect of TTR against Aβ toxicity has been observed in vitro[5−8] and supported by other animal studies. For example, progeny from APP_{Sw} mice crossed with mice engineered to express human TTR performed as well as wild-type and better than APP_{Sw} mice in cognitive tests,[9] and AD mice raised in an enriched environment expressed more TTR and performed better on cognitive tests than those raised in a control environment.[10]

Received: February 8, 2013
Revised: March 21, 2013
Published: April 9, 2013

TTR is a 55 kDa homotetrameric transport protein that is synthesized in the liver and choroid plexus and is present in both blood (3−7 μM) and cerebrospinal fluid (CSF, 0.1−0.4 μM).[11,12] Each monomer contains two four-stranded β-sheets, an inner sheet of strands D, A, G, and H, and an outer sheet of strands C, B, E, and F, as well as a short α-helix and loop between strands E and F. The assembly of the monomer into dimers is stabilized by extensive hydrogen bonding. The assembly of dimers into tetramers occurs via a small contact region between the AB loop and H strands. Tetramer assembly creates a hydrophobic pocket in which thyroxine binds. TTR is the primary carrier for thyroxine in CSF and a secondary carrier in blood, with ∼15−20% of TTR containing thyroxine. TTR also serves as carrier for retinol-binding protein (RBP), which binds near residues in the EF loop. RBP and thyroxine do not compete for binding to TTR, and both ligands reportedly stabilize TTR tetramers and reduce the levels of TTR misfolding and aggregation.

We and others have shown that TTR binds to Aβ.[13−15] L82 and L110 were identified as two critical residues on TTR that mediate the interaction between Aβ and TTR.[13] L82 is on the EF helix/loop, while L110 is in strand G, part of the inner sheet that lines the hydrophobic thyroxine-binding pocket (Figure 1).

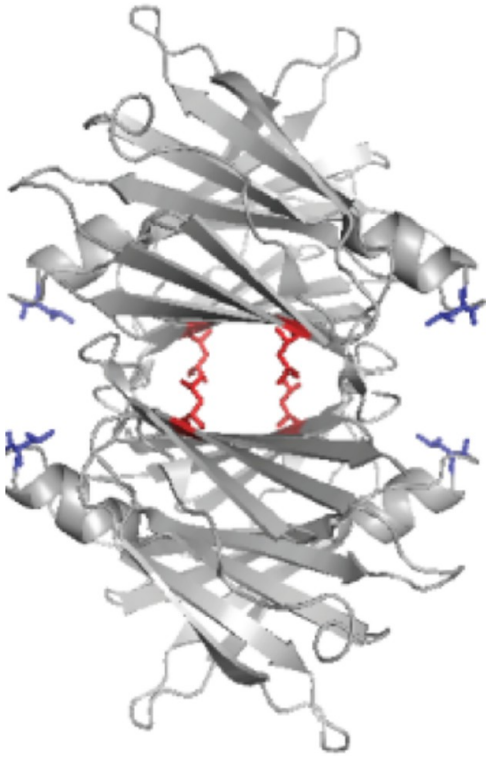

Figure 1. Ribbon structure of TTR tetramers, showing Leu82 (blue, on end of the EF helix) and Leu110 (red, on strand G). Mutation of either of these leucines to alanine resulted in significantly less binding of Aβ.[13]

The level of binding of Aβ to alanine mutants L82A and L110A was significantly reduced compared to that of wild-type TTR.[13] In this study, we used these mutants to further elucidate the mode of interaction between Aβ and TTR and the means by which TTR mediates protection against Aβ-induced neuronal toxicity.

EXPERIMENTAL PROCEDURES

TTR Production and Purification. Recombinant human transthyretin was produced and purified as previously described in detail.[13] The wild type (wt) and three mutants were prepared: F87M/L110M (mTTR), L82A, and L110A. F87M/L110M is an engineered TTR mutant that is stable as a monomer.[16] L82A and L110A are mutants with nativelike secondary, tertiary, and quaternary structure, but both show substantially decreased levels of binding of Aβ relative to that of wt.[13]

***In Vitro* Cellular Toxicity.** Primary cortical neuronal cultures were generated from individual E15.5 embryos derived from C57/Bl6 female mice. Briefly, individual cortices were dissected and dissociated with trypsin and plated on individual poly-D-lysine-coated 96-well plates or on coverslips in 24-well plates at a density of 100000 or 400000 cells/well, respectively. Cells were initially plated in modified Eagle's medium containing fetal bovine serum, horse serum, L-glutamine, and penicillin/streptomycin (PS). After 45 min, the medium was replaced with neurobasal medium (NBM) supplemented with B27, PS, and L-glutamine for the duration of the experiment in the humidified tri-gas incubator under normoxic conditions. Half of the NBM was changed with fresh NBM every 2−3 days. Aβ(1−42) (American Peptide, Sunnyvale, CA) at 1 mg/mL was prepared in phosphate-buffered saline (PBS) and then diluted to a final concentration of 10 μM with wt or mutant TTR (mTTR, L82A, and L110A) for 1 h in NBM supplemented with B27 without the antioxidant, L-glutamine, and PS. The TTR/Aβ mixture was then added to cells after 6 days *in vitro* (DIV), and viability was assessed after 8 DIV.

The MTS [3-(4,5-dimethylthiazol-2-yl)-5-(3-carboxymethoxyphenyl)-2-(4-sulfophenyl)-2*H*-tetrazolium salt] assay (Promega) was used according to the manufacturer's instructions to assess cell viability. Briefly, phenazine methosulfate (PMS) and MTS were mixed together at a 1:20 ratio immediately before being used. Twenty microliters of MTS/PMS mixture was added per well of a 96-well plate and incubated with cells for 2 h in the humidified tri-gas incubator. The quantity of resulting formazan product was measured by 490 nm absorbance on a UV−vis plate reader. Triplicate measurements were taken under each condition; data are reported relative to medium-treated cells.

To assess apoptotic cell death, terminal deoxynucleotidyl-transferase-mediated dUTP nick end labeling (TUNEL; *in situ* cell death detection kit, TMR red; Roche) was employed by following the manufacturer's instructions. Apoptotic cells were identified by fluorescein labeling of DNA strand breaks with the TdT enzyme. Briefly, cells on coverslips were washed and fixed in 4% paraformaldehyde for 60 min. Following three washes, the cells were permeabilized with freshly prepared 0.1% Triton X-100 in 0.1% sodium citrate for 2 min on ice; 50 μL of the enzyme solution and 450 μL of the label solution from the kit were mixed together and incubated with the cells in a humidified chamber for 1 h. Positive and negative controls were run along with the samples. The cells were washed postincubation and mounted on the glass slides with aqueous mounting medium containing DAPI to counterstain the nuclei. The samples were visualized using a Zeiss fluorescence microscope with 595 nm emission for TUNEL and 350 nm emission for DAPI.

Peptide Arrays. A series of peptides with overlapping sequences derived from Aβ, each 10 amino acids long, was

synthesized onto a cellulose membrane (Sigma-Genosys, St. Louis, MO). The membrane was wetted with a few drops of methanol, rinsed with water, and then washed with 10 mL of Tris-buffered saline (TBS) [20 mM Tris and 150 mM NaCl (pH 7.6)] three times for 10 min each. After overnight incubation in casein blocking buffer (Thermo Scientific), the membrane was washed with 10 mL of TBS and incubated with 10 mL of TTR or mTTR (5 μg/mL in blocking buffer) at room temperature overnight. The membrane was washed three times with 10 mL of T-TBS [TBS with 0.05% (v/v) Tween 20] for 10 min each, and bound protein was transferred onto a 0.2 μm poly(vinylidene difluoride) (PVDF) membrane (Millipore Corp., Billerica, MA) at 70 mA three times (for 30, 30, and 60 min). The three PVDF membranes were blocked with 10 mL of blocking buffer overnight and then reacted with the anti-human TTR antibody (DAKO, Glostrup, Denmark) at a 1:1500 dilution in blocking buffer for 2 h. PVDF membranes were subsequently treated with the anti-rabbit immunoglobulin/HRP antibody (DAKO) at a 1:1500 dilution in blocking buffer for 2 h. Bound TTR was visualized by means of the ECL Western Blotting Analysis System (GE Healthcare, Buckinghamshire, U.K.).

Enzyme-Linked Immunosorbent Assay (ELISA) Measurement of Aβ−TTR Binding. ELISA plates (Corning Inc., Corning, NY) were coated with 5 μg/mL wt TTR (100 μL/well) in coating buffer [10 mM sodium carbonate, 30 mM sodium bicarbonate, and 0.05% NaN_3 (pH 9.6)] overnight at room temperature. The plate was washed three times with phosphate-buffered saline (PBS) [10 mM Na_2HPO_4/NaH_2PO_4 and 150 mM NaCl (pH 7.4) with 0.05% Tween 20] and incubated with blocking buffer (5% nonfat dry milk in PBS-T) for 2 h at room temperature. For a negative control, TTR was not coated, but wells were incubated with blocking buffer. Four replicate wells were prepared under each condition. The Aβ stock solution was prepared by dissolving lyophilized Aβ [Aβ(1−40) (Anaspec, Inc., San Jose, CA)] to a final concentration of 2.8 mM in 8 M urea (pH 10) as described previously.[17] Aβ samples were prepared by dilution of the Aβ stock into PBS with 0.02% sodium azide to a final concentration of 0.8 mg/mL. Freshly prepared Aβ or Aβ aggregated for 1−7 days was diluted to 5 μg/mL in PBS and then immediately added to TTR-coated or control wells (50 μL/well). The plate was incubated at 37 °C for 1 h. After the sample had been washed, anti-Aβ antibody 6E10 [1:3000 in PBS-T (Covance, Princeton, NJ)] was added to each well (100 μL/well), and the plate was incubated at room temperature for 1 h while being gently shaken. After the sample had been washed, the anti-mouse HRP antibody [1:3000 dilution (Pierce, Rockford, IL)] was added to each well (100 μL/well), and the plate was incubated for 1 h at room temperature while being gently shaken. The plate was washed three times, and then 100 μL of a 3,3′,5,5′-tetramethylbenzidine (TMB) substrate solution (Pierce) was added to each well. The plate was incubated at room temperature for 15−30 min; color development was stopped by adding 100 μL of 2 M sulfuric acid. Absorbance was measured at 450 nm with an EL800 Universal Microplate Reader (Biotek Instruments Inc., Winooski, VT). Aβ binding was calculated as the mean of four replicate wells by subtracting the absorbance of the negative control from the sample absorbance.

Immunoblot Assays. Aβ (28 μM) in PBS was mixed with 0.5 μM TTR and incubated for up to 24 h at room temperature; 1.5 μL was dotted onto a 0.45 μm nitrocellulose membrane (Pierce) after incubation for 0, 5, and 24 h. The dried membrane was blocked with 5% nonfat dry milk in T-TBS overnight at 4 °C and reacted with the OC antibody (Millipore Corp.) diluted to 1:2000 in 5% nonfat dry milk in T-TBS for 1 h at room temperature. After being washed three times with T-TBS, the membrane was incubated with the anti-rabbit immunoglobulin/HRP antibody diluted to 1:1000 in 5% nonfat dry milk in T-TBS for 30 min at room temperature. After being washed, the membrane was visualized by means of the ECL Western Blotting Analysis System.

Photoinduced Cross-Linking of Aβ. The photoinduced cross-linking of the unmodified protein (PICUP) experiment was performed according to the protocol of Fancy and Kodadek[18] with some modifications. Aβ samples at different aggregation states were prepared by dilution to 0.8 mg/mL in PBS from an Aβ stock and incubation at room temperature for 0−7 days. Aβ samples were then diluted to 30 μM in PBS prior to PICUP analysis. One microliter of 1 mM tris(2,2′-bipyridyl)dichlororuthenium(II) (Sigma) and 1 μL of 20 mM ammonium persulfate (Sigma) in PBS were added to an 18 μL sample. The cross-linking reaction was conducted by irradiation with visible light for 10 s, and the reaction was quenched immediately by addition of 1 μL of 1 M DTT. A flashlight (Mag-lite) with a krypton lamp was used as a light source, and the reaction mixture in the tube was placed parallel to the beam of light at a distance of 5 cm. Samples were separated by SDS−PAGE on a Precise 4 to 20% polyacrylamide gradient gel (Pierce) and transferred onto a 0.45 μm nitrocellulose membrane (Pierce) at 60 V for 1 h. The membrane was blocked with 5% nonfat dry milk in T-TBS overnight at 4 °C, washed three times with T-TBS, and reacted with the 6E10 antibody diluted to 1:7500 in T-TBS for 1 h at room temperature. After being washed, the membrane was incubated with the anti-mouse HRP antibody diluted to 1:7500 in T-TBS for 30 min at room temperature. After being washed for 30 min, the membrane was visualized by means of the ELC Western Blotting Analysis System.

Dynamic Light Scattering (DLS). All buffers and TTR samples were filtered through 0.02 μm filters before being used. Lyophilized Aβ(1−40) (Anaspec, Inc.) was dissolved in a 8 M urea/0.01 M glycine-NaOH mixture (pH 10)[17] to a final concentration of 2.8 mM, then snap-frozen, and stored at −80 °C. Immediately before each experiment, frozen stocks were thawed and sonicated for 2 min before being diluted into PBSA. Aβ alone (23 μM) or mixed with TTR (7 μM) was filtered through a 0.45 μm filter directly into a light scattering cuvette and then placed into a bath of the index-matching solvent decahydronaphthalene with the temperature controlled to 25 °C. Light scattering data were collected using a Brookhaven BI-200SM system (Brookhaven Instruments Corp., Holtsville, NY) and an Innova 90C-5 argon laser (Coherent, Santa Clara, CA) operating at 488 nm and 150 mW. The z-averaged hydrodynamic diameter was determined from the autocorrelation function using the method of cumulants.

Nanoparticle Tracking (NTA). NTA measurements were taken with a Nanosight LM10 (Nanosight, Amesbury, U.K.) equipped with a 405 nm laser. All buffers were filtered through 0.02 μm filters prior to use as were TTR samples. Aβ solutions were prepared as described for DLS. Aβ alone (28 μM in PBSA) or mixed with TTR (0.7 μM) was injected into the sample chamber using a syringe. All measurements were collected at room temperature with the camera level set to the maximal value to allow for the detection of smaller particles.

One 90 s video was taken every 30 min for 6 h and then hourly for an additional 18 h. Data were captured and analyzed using NTA version 2.3.

Native Gel Electrophoresis. TTR alone (3.6 μM) or with Aβ (82 μM) was incubated for 0 or 2 days at 25 or 37 °C and then diluted in SDS to a final concentration of 2% (w/v). Samples were loaded on a Precise 4 to 20% polyacrylamide gradient gel (Pierce) along with EZ-Run Protein Ladder (Fisher BioReagents, Fair Lawn, NJ) and electrophoresed using SDS buffer for 45 min at 125 V. Gels were stained with Coomassie blue. TTR tetramers are normally stable under these electrophoresis conditions.

Circular Dichroism (CD) Analysis. TTR stock solutions were dialyzed against phosphate/NaF buffer [10 mM Na_2HPO_4/NaH_2PO_4 and 150 mM NaF (pH 7.4)]. TTR alone (3.6 μM) or with Aβ (82 μM) was incubated for 0−2 days at 37 °C. Samples were then diluted 6-fold and transferred into a 1 mm cell. CD spectra were collected on an Aviv 202SF CD spectrophotometer from Aviv Biomedical (Lakewood, NJ) at 22 °C. Blank solvent spectra and spectra for Aβ alone were collected and subtracted.

Cross-Linking and Analysis by Gel Electrophoresis and Western Blotting. Fifty microliters of TTR alone (3.6 μM) or TTR with Aβ (82 μM) in PBS was incubated for 2 h at 37 °C and cross-linked with glutaraldehyde by adding 2 μL of a 25% glutaraldehyde solution. After 2 min, 2 μL of 7% (w/v) $NaBH_4$ in 0.5 M NaOH was added to quench the reaction. The samples were heated at 95 °C for 5 min and analyzed on a Precise 4 to 20% polyacrylamide gradient gel (Pierce). One gel was stained with Coomassie blue. A second gel was transferred onto 0.45 μm nitrocellulose membranes (Pierce) at 60 V for 1 h. Membranes were blocked with 5% nonfat dry milk in T-TBS overnight at 4 °C. After being washed three times with T-TBS, the membrane was incubated with the anti-human TTR antibody at a 1:1500 dilution in T-TBS and then with the anti-rabbit immunoglobulin/HRP antibody at a 1:1500 dilution in T-TBS. After being washed, membranes were visualized by means of the ECL Western Blotting Analysis System (GE Healthcare).

TTR Tetramer Dissociation Kinetics. The S-Trap method was used to measure the rate of tetramer dissociation.[19] TTR (0.4 mg/mL in PBSA) was diluted with SDS buffer [25% glycerol, 2% SDS, 0.01% bromophenol blue, and 62.5 mM Tris-HCl (pH 6.8)] so that the final concentrations of protein and SDS were 0.2 mg/mL (3.6 μM) and 1%, respectively. SDS buffer was preheated at 90 °C to quickly achieve the desired temperature (80 °C) after mixing. After incubation for different periods of time, the samples were quickly placed in an ice/water bath for 5−10 s and then centrifuged for 5 s at 3000 rpm. Samples were loaded on a Precise 4 to 20% polyacrylamide gradient gel (Pierce) along with EZ-Run Protein Ladder (Fisher Bioreagents) and electrophoresed for 45 min at 125 V. Gels were stained with Coomassie blue. Destained gels were photocopied, and the images were analyzed using ImageJ. The fraction of unfolded protein was determined by the ratio between the amount of unfolded and total protein. The tetramer dissociation rate (k_d) was obtained by fitting the fraction of unfolded protein versus incubation time to a single-exponential equation.

RESULTS

Loss of Binding Sites Reduces the Level of TTR Protection against Aβ Toxicity. In cortical cultures exposed to 10 μM Aβ, we observed a reduction to 50% cell viability as measured by the MTS assay (Figure 2a). wt TTR protected Aβ toxicity in a dose-dependent manner, achieving complete protection at ∼6 μg/mL (∼0.1 μM), or a 1:100 TTR:Aβ molar ratio (Figure 2), consistent with previously reported data from our own laboratory and others.[7,20,21] A stable monomeric mutant, F87M/L110M (mTTR), also afforded complete protection against Aβ toxicity at ∼3 μg/mL (∼0.2 μM). Both wt and mTTR bind Aβ, with stronger binding of Aβ to mTTR than wt.[14] In previous work, leucine residues L82 and L110 on TTR (Figure 1) were identified as being important contributors to TTR−Aβ association, and binding of Aβ to TTR alanine mutants L82A and L110A was significantly weakened compared to wt binding, despite the fact that these mutants retained native secondary, tertiary, and quaternary structure.[13] L82A and L110A were much less effective at protecting neurons against Aβ toxicity (Figure 2a). In control experiments, TTR alone (wt, mTTR, L82A, or L110A) had no effect on cell viability (data not shown).

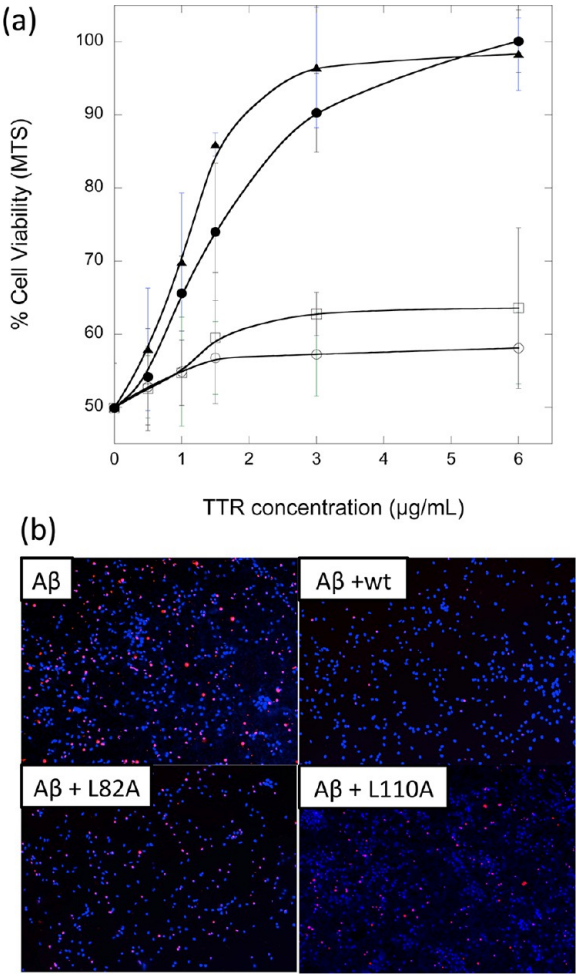

Figure 2. Effect of TTR on Aβ toxicity. (a) Neuron-enriched cortical cultures were established from mouse embryos and then exposed to Aβ alone (10 μM) mixed with varying concentrations of wt TTR (●), mTTR (▲), L82A (○), and L110A (□). Viability was assessed relative to that of vehicle-treated cells using MTS. (b) Cells were exposed to Aβ alone (top) or Aβ with wt, L82A, or L110A and then assessed for apoptosis using TUNEL staining.

dx.doi.org/10.1021/bi4001613 | *Biochemistry* 2013, 52, 2849−2861

TUNEL staining was used to corroborate the MTS results. Apoptotic cells are clearly present in the Aβ-treated cortical cultures, as evidenced by red staining of DNA strand breaks (Figure 2b). The addition of wt TTR to Aβ virtually eliminated red staining. However, neither L82A nor L110A was effective at preventing Aβ-mediated apoptosis. These results connect the loss of binding sites on TTR to a reduction in TTR's ability to inhibit Aβ toxicity, demonstrate that binding of Aβ to TTR is causally linked to TTR-mediated protection, and support the role of leucine residues L82 and L110 in mediating biologically relevant Aβ−TTR association.

Aβ Soluble Aggregates Bind Preferentially to TTR. In previous work, we synthesized peptide arrays containing linear sequences of TTR and used these arrays to identify specific sequences, corresponding to strand G and the EF helix/loop, to which soluble Aβ bound.[13] In an attempt to identify residues on Aβ that contribute to TTR−Aβ binding, we reversed the experiment and constructed peptide arrays containing linear sequences of Aβ 10 residues long. Despite repeated attempts, we observed no binding of either TTR or mTTR to any spots on the peptide arrays (data not shown). Using anti-Aβ antibodies directly, we were able to easily detect spots, indicating that the peptides were correctly synthesized and were available for binding. Possible (nonexclusive) explanations for this result include (a) that the TTR binding site on Aβ is noncontiguous, (b) that a specific conformation of Aβ is required for TTR binding, and/or (c) that Aβ must be aggregated to bind to TTR.

To test whether Aβ must be in a specific conformation or state of aggregation to bind TTR, we incubated Aβ for 0−7 days and then characterized its binding to TTR by ELISA and its aggregation state by cross-linking and gel electrophoresis. Freshly prepared Aβ bound poorly to TTR-coated wells (Figure 3a), consistent with previous observations.[14] The level of binding increased for samples aggregated for 1−5 days prior to contact with TTR but then partially decreased if Aβ was aggregated for 7 days (Figure 3a). Cross-linking studies revealed that freshly prepared Aβ contained only low-molecular mass oligomers [primarily apparent dimers and trimers with some monomers and tetramers (Figure 3b)]. On day 1, some high-molecular mass aggregates (>100 kDa) were in evidence, along with low-molecular mass oligomers. The distribution between low-molecular mass oligomers and high-molecular mass aggregates remained roughly constant from day 1 through day 5. On day 7, the Aβ sample was very viscous, and much of the material did not enter through the gel, indicative of a highly aggregated population. The level of low-molecular mass oligomers was substantially diminished. All samples stained positive with the OC antibody (not shown), a conformationally specific antibody that detects soluble and insoluble fibrillar aggregates.[22] From the combined data, we conclude that soluble fibrillar Aβ aggregates (≳100 kDa) bind much more to TTR than low-molecular mass oligomers, but that very mature, highly aggregated Aβ binds poorly to TTR.

TTR Slows the Aggregation of Aβ. We tested the effect of TTR (wt, L82A, and L110A) on the growth of Aβ aggregates, using dynamic light scattering. For these experiments, we used snap-frozen and thawed Aβ samples. Aβ prepared in this manner contains some aggregates initially. Experiments were conducted at a moderate (~3:1) molar Aβ excess, to accentuate the effect of TTR. Growth rates were monitored for 45 min. The fastest growth rate, as measured by the increase in the mean hydrodynamic diameter of aggregates,

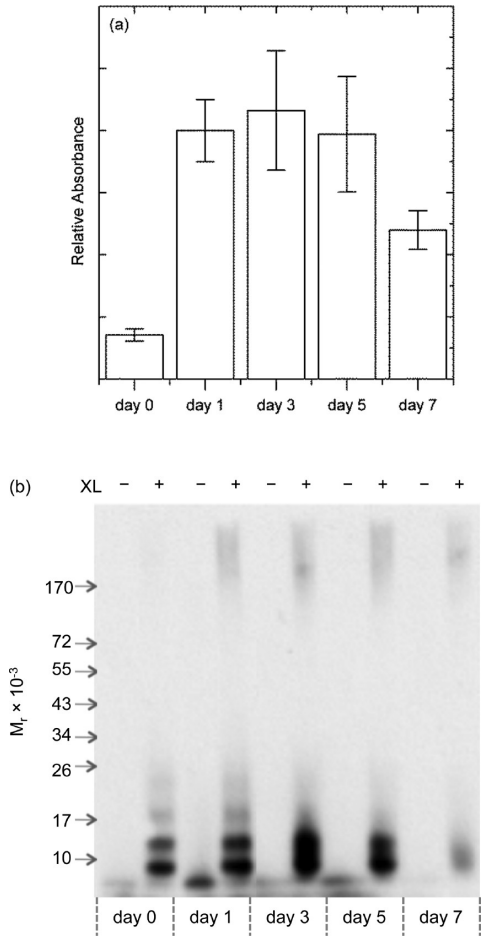

Figure 3. Effect of Aβ aggregation state on binding to TTR. (a) Relative amount of Aβ bound to immobilized TTR, as determined by an ELISA. Aβ was freshly prepared (day 0) or preaggregated for the indicated number of days prior to its contact with TTR. (b) Size distribution of Aβ as function of the number of days aggregated, ascertained by PICUP cross-linking and gel electrophoresis.

was observed with Aβ alone. wt TTR significantly slowed the rate of growth, as did L110A. L82A was less effective at slowing the initial growth rate than L110A (Figure 4).

Nanoparticle Tracking Measures Aβ Aggregate Size Distribution and Number Concentration. We here introduce the use of nanoparticle tracking analysis (NTA) to detect Aβ aggregates and measure the growth of aggregates over time. To the best of our knowledge, this is the first reported use of NTA to monitor Aβ aggregation. Briefly, in NTA, scattering from individual particles is detected and the trajectory of those particles is tracked over a short time, from which a diffusion coefficient and an equivalent hydrodynamic diameter are calculated.[23] Nanoparticle tracking has advantages over conventional DLS for several reasons: a particle number concentration can be measured, smaller and weaker scatterers are detected even in the presence of larger and stronger scatterers, and a size distribution is directly obtained because single particles are tracked. NTA has some advantages over AFM: particles remain in solution, so surface effects are not a significant concern. There are some limitations as well; in particular, smaller (<50 nm) particles cannot be reliably tracked, so Aβ monomers or smaller Aβ oligomers are not measured.

dx.doi.org/10.1021/bi4001613 | Biochemistry 2013, 52, 2849−2861

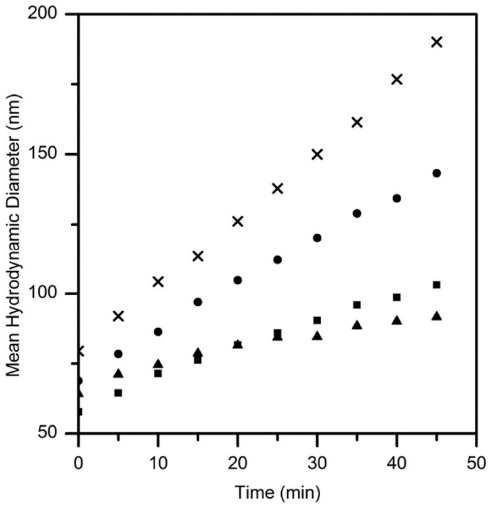

Figure 4. Effect of TTR (wt and mutants) on Aβ aggregate growth kinetics. The mean hydrodynamic diameter of aggregates was measured by dynamic light scattering. Samples contained 23 μM Aβ alone (×) or Aβ with 7 μM wt (■), with L82A (●), or with L110A (▲).

We first checked the buffer only. No aggregates were detected in these samples: the video was completely dark (not shown). We next collected data for a solution of Aβ (28 μM) at several time points, up to 24 h. Particle counts at each particle size (1 nm resolution) are summed and converted to the number of particles per milliliter. Representative size distributions at 0.5 and 12 h are shown in Figure 5a. With time, the number of particles increased, and the size distribution broadened and shifted toward larger aggregates. The absence of <50 nm particles is due to limitations in detecting and tracking smaller aggregates; because of this, the mean size of aggregates detected by NTA is larger than that detected by DLS. By modeling the aggregates as wormlike chains with 100 nm persistence lengths and 10 nm diameters,[17] we estimated that ~3% of the total mass of Aβ is incorporated into these large aggregates (>50 nm hydrodynamic diameter, or ~200 nm or longer contour length) at early times, increasing to ~8% after 24 h. To simplify the presentation of the data, we binned particles (50 nm bin size for diameters of <400 nm, 100 nm bin size for diameters of >400 nm). Figure 5b illustrates binned size distributions for Aβ aggregates taken at four time points. The growth in both the number and the size of aggregates over time is evident.

TTR Affects the Aβ Aggregate Size Distribution and Number Concentration. We first confirmed that TTR did not contribute any signal to the NTA measurement. Aβ was mixed with TTR (wt, L82A, or L110A) in PBSA, and the effect of TTR on Aβ aggregation was evaluated using NTA. The addition of wt TTR completely arrested the growth of aggregates: the size distribution did not change (Figure 6), and the particle number concentration did not increase (Figures 6 and 8), for at least 12 h. These data show that wt TTR effectively suppresses both the growth in the size of preexisting aggregates and the appearance of new aggregates.

We next compared the effect of L82A and L110A on Aβ aggregation to that of wt TTR. Although both mutants had some effect on slowing the growth of Aβ aggregates, neither was as effective as wt (Figure 7). Unlike with wt, the size distribution shifted toward larger aggregates, albeit less than

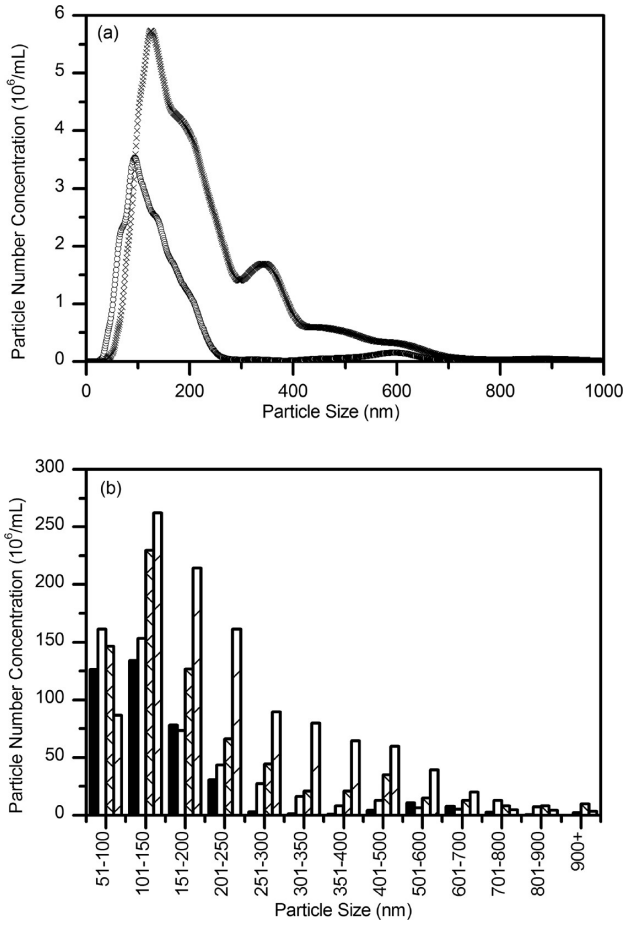

Figure 5. Nanoparticle tracking analysis of Aβ aggregate growth kinetics. Aβ (28 μM) was prepared in PBSA from stock solutions and incubated at room temperature. (a) Size distribution of Aβ aggregates after 0.5 h (○) and after 12 h (×). Distributions are shown at 1 nm resolution. (b) Size distributions of Aβ aggregates were binned and compared after incubation for 0.5 (black), 3.5 (white), 7 (cross-hatched), and 12 h (striped).

with Aβ alone (Figure 7a–d). Over time, L110A was less effective than L82A at suppressing Aβ growth. This is the opposite of the behavior observed in DLS, but those data were taken over only 45 min.

The total particle number concentration versus time is shown in Figure 8. This analysis again illustrates that Aβ aggregates grow in number over time, that wt completely prevents new aggregates from forming (aggregates of the size that can be detected by NTA), and that both L82A and L110A partially suppress growth in particle number, but not as effectively as wt.

Aβ preparations used in these experiments were characterized by immunoblotting. Two conformationally specific polyclonal antibodies were used. OC binds to soluble fibrillar oligomers and fibrils, including both thioflavin S-positive and -negative deposits.[24] The level of OC-positive deposits is significantly higher in AD than age-matched controls and increases with the severity of dementia, and the level of OC-positive staining increases dramatically in Tg2576 but not wt mice after 12 months.[25] A11 reportedly binds to "prefibrillar oligomers" but not to fibrillar oligomers or mature fibrils.[26] Our Aβ samples were OC-positive and A11-negative. The addition of TTR did not affect the OC-positive status, despite the deceleration in the aggregation rate (Figure 8). This result

dx.doi.org/10.1021/bi4001613 | Biochemistry 2013, 52, 2849–2861

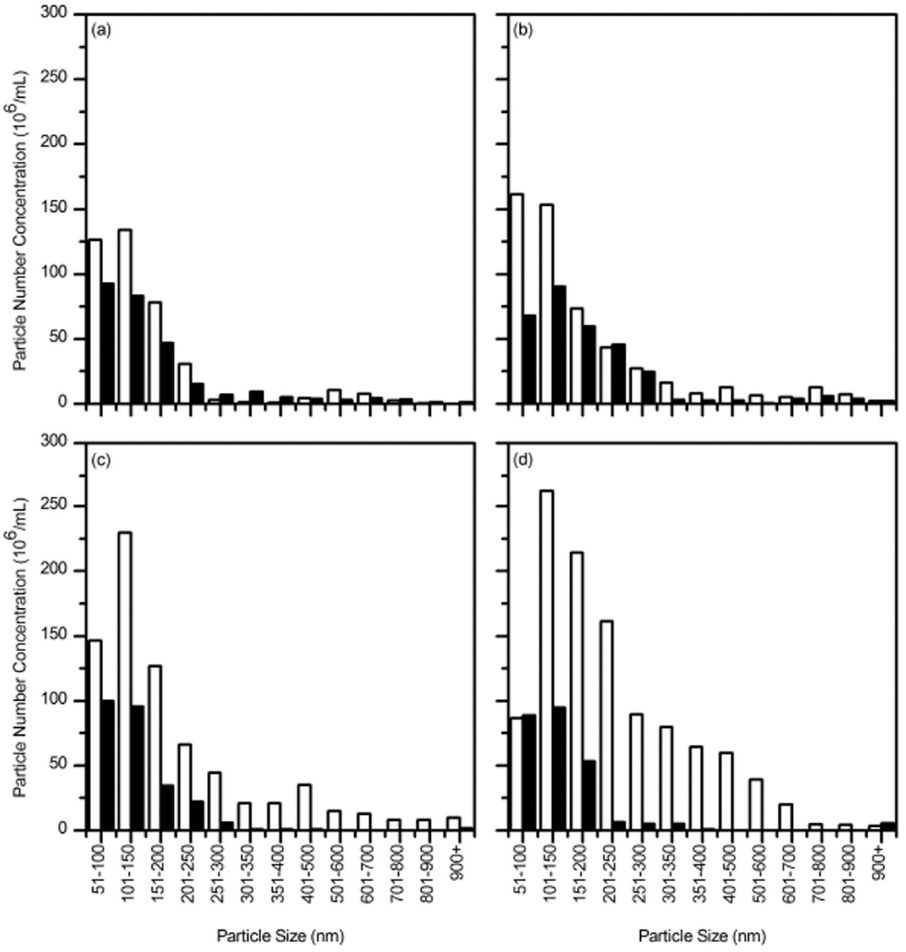

Figure 6. Size distributions of Aβ alone (white bars) or Aβ incubated with wt TTR (black bars) as a function of incubation time, as measured by NTA: (a) 0.5, (b) 3.5, (c) 7, and (d) 12 h.

suggests that TTR binding does not cause a significant change or rearrangement in the conformation of Aβ aggregates.

Binding of Aβ Triggers a Conformational Change in TTR. We incubated TTR (wt, L82A, and L110A) with Aβ for up to 2 days and collected CD spectra for these mixtures as well as for Aβ or TTR alone. We subtracted the spectra for Aβ alone from that for TTR with Aβ and then compared the CD spectra for TTR alone to that for TTR in the presence of Aβ. Spectra for wt, L82A, and L110A were very similar, as reported previously,[13] indicating no changes in secondary structure are caused by the alanine mutations. On day 0, we saw no change in the TTR spectra in the presence of Aβ (data not shown). After incubation for 2 days, however, we observed a measurable shift in the spectra for wt TTR in the presence of Aβ (Figure 9). In contrast, CD spectra of L82A or L110A were minimally affected by Aβ (Figure 9). For comparison, we produced two TTR mutants: F87M/L110M, an engineered TTR mutant that is stably monomeric, and S112I, a dimeric mutant. We compared CD spectra for these two mutants (without Aβ) to those of wt TTR. The CD spectra for the monomeric and dimeric TTR variants are shifted upward (less negative ellipticity) relative to those of wt, similar to the shift observed for wt TTR in the presence of Aβ (data not shown). A similar upward shift in CD spectra was previously reported for the TTR mutant S85A, which assembles into unstable tetramers.[13]

We considered two possible explanations for these results. First, binding of Aβ could induce a change in wt TTR structure, leading to destabilization of the tetramer. Weaker binding of Aβ to L82A and L110A could be insufficient to trigger this destabilization, and/or binding to both sites could be required for destabilization. Alternatively, the Aβ secondary structure could be changed because of TTR binding, so subtraction of the spectra for Aβ alone from the spectra for wt with Aβ does not correctly account for the contribution of Aβ to the spectra. We tested the first hypothesis by looking for other evidence of tetramer destabilization.

Aβ Binding Facilitates TTR Tetramer Destabilization and/or Dissociation. TTR is natively a very stable tetramer, but it undergoes slow monomer and dimer subunit exchange, with half-times on the order of 18−24 h.[27] To explore whether TTR tetramer stability is affected by Aβ, we incubated TTR (wt, L82A, and L110A) alone or with Aβ at room temperature for 0, 1, or 2 days and then analyzed samples by native gel electrophoresis, under conditions where TTR normally runs as a tetramer and Aβ as a monomer. As expected, TTR alone (wt or mutant) was tetrameric and remained tetrameric for 2 days (Figure 10). When Aβ was added to TTR and the sample was analyzed shortly after being mixed, bands corresponding to the TTR tetramer and Aβ monomer were observed, as expected (Figure 10a). After co-incubation for 1 day (not shown) or 2 days (Figure 10b), however, partial dissociation of TTR tetramers to monomers was observed for wt and L110A, but not for L82A. Similar results were obtained with incubation at 37 °C (not shown).

dx.doi.org/10.1021/bi4001613 | *Biochemistry* 2013, 52, 2849−2861

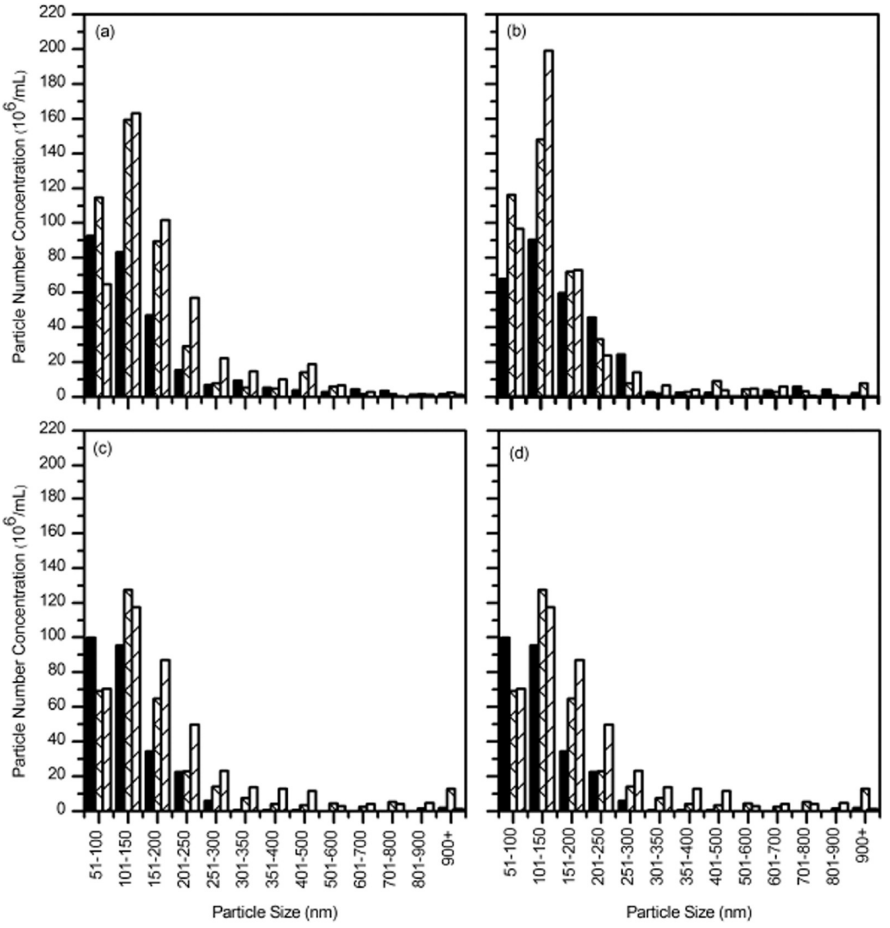

Figure 7. Size distributions of Aβ with wt TTR (black), Aβ with L82A (cross-hatched), and Aβ with L110A (striped) as a function of incubation time, as measured by NTA: (a) 0.5, (b) 3.5, (c) 7, and (d) 12 h.

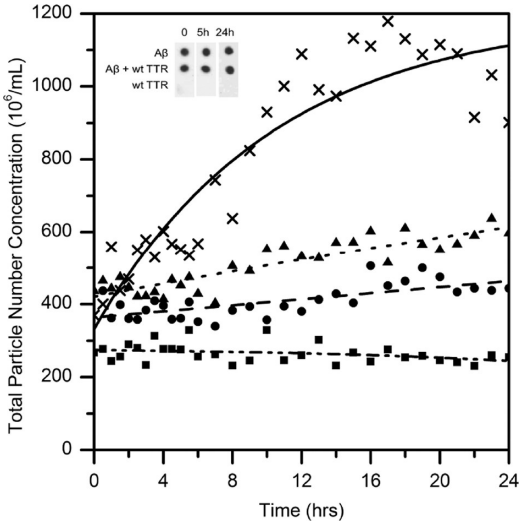

Figure 8. Total aggregate number concentration as a function of time, as measured by NTA. Aβ was incubated alone (×) or with wt TTR (■), L82A (●), or L110A (▲). The inset shows immunoblots of Aβ mixed with and without wt TTR and stained with the OC antibody.

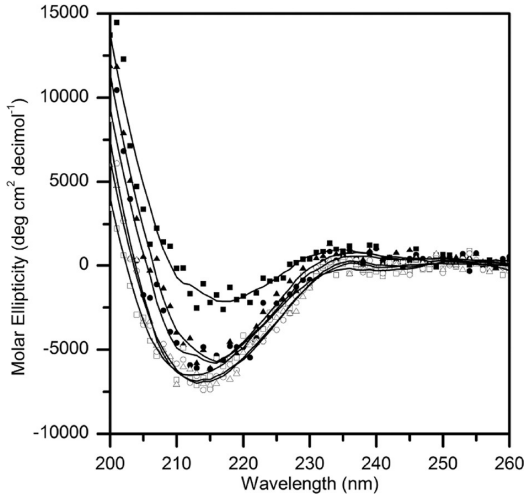

Figure 9. CD spectra of TTR alone (empty symbols) or after incubation with Aβ for 2 days (filled symbols). Buffer spectra were subtracted from those of TTR alone, while CD spectra of Aβ in buffer were subtracted from those of TTR with Aβ: wt (□), L82A (○), L110A (△), wt with Aβ (■), L82A with Aβ (●), and L110A with Aβ (▲).

We next explored why Aβ destabilized wt and L110A, but not L82A. We previously showed that L110A and L82A mutations did not cause a loss of secondary, tertiary, or quaternary structure in TTR.[13] We tested whether these mutations caused a more subtle effect on tetramer stability by measuring dissociation at high temperatures using the S-Trap method.[19] This method prevents reassociation or aggregation of the dissociated monomer. Dissociation rate constants (k_d) for wt and L82A were indistinguishable (Table 1), and the rate

dx.doi.org/10.1021/bi4001613 | *Biochemistry* 2013, 52, 2849−2861

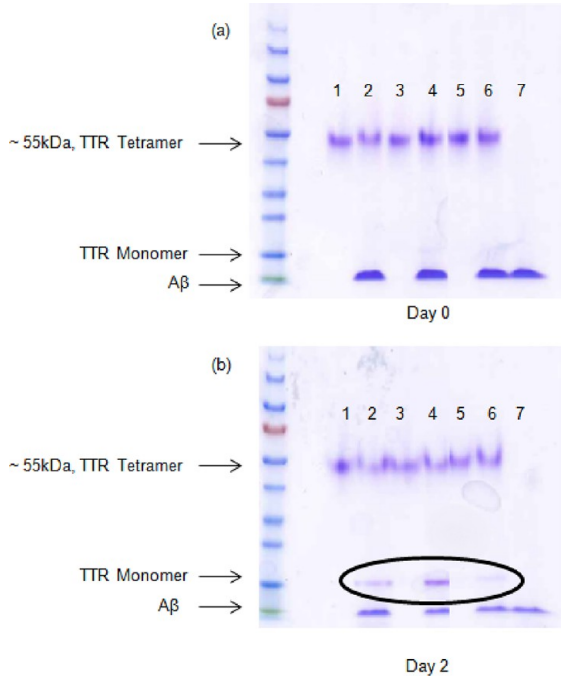

Figure 10. Native gel electrophoretic analysis of TTR tetramer stability without and with Aβ over time: (a) 0 days at 25 °C and (b) 2 days at 25 °C. Lanes 1, 3, and 5 contained wt, L110A, and L82A without Aβ, respectively. Lanes 2, 4, and 6 contained wt, L110A, and L82A with Aβ, respectively. Lane 7 contained Aβ alone.

Table 1. Comparison of wt and Mutant TTR Tetramer Dissociation Rates at 80 °C, Measured Using the S-Trap Method[a]

	k_d (min^{-1})	[$t_{1/2}$ (min)]
wt	0.31 ± 0.04	[2.2 ± 0.2]
L82A	0.30 ± 0.03	[2.3 ± 0.2]
L110A	0.42 ± 0.05	[1.6 ± 0.2]

[a]Both the first-order rate constant (k_d) and the half-time ($t_{1/2}$) are reported.

constant for wt is consistent with published data.[19] Thus, the lack of tetramer dissociation for L82A incubated with Aβ is not due to an increase in the stability of L82A relative to that of wt. With L110A, k_d increased by roughly 30%. Thus, there is a modest reduction in the tetramer stability of L110A that may account, in part, for the enhanced dissociation of L110A in the presence of Aβ.

To see if Aβ is simply acting nonspecifically, like a detergent, and trapping TTR monomers during subunit exchange, we incubated TTR (wt and mutants) with SDS (either 0.5 or 2%) for 0 or 2 days. On day 0, the protein was fully a tetramer, as expected, but after 2 days, a significant fraction was dissociated into monomers. The monomer:tetramer ratio was approximately the same for all three proteins [wt, L110A, and L82A (data not shown)]. This result indicates that Aβ is acting specifically, because Aβ affects each TTR mutant differently whereas SDS has similar effects on all mutants.

To see if the lag in formation of TTR monomers in the presence of Aβ could be attributed to the time it takes to form Aβ aggregates, we preaggregated Aβ for 1−2 days prior to adding TTR. After co-incubation of TTR with preaggregated Aβ for 1 h, we observed no TTR monomer bands (data not shown). These data show that the slow appearance of the TTR monomer bands is not due to the time scale for Aβ aggregation but rather to slow TTR tetramer dissociation.

We conducted a similar experiment in which Aβ and TTR were incubated and then analyzed by gel electrophoresis, except we cross-linked with glutaraldehyde before running the gels and boiled the samples prior to application to the gel. Under these conditions, TTR runs as a monomer in the absence of a cross-linker. Gels were analyzed by Coomassie staining as well as Western blots with anti-TTR antibodies (Figure 11). With wt

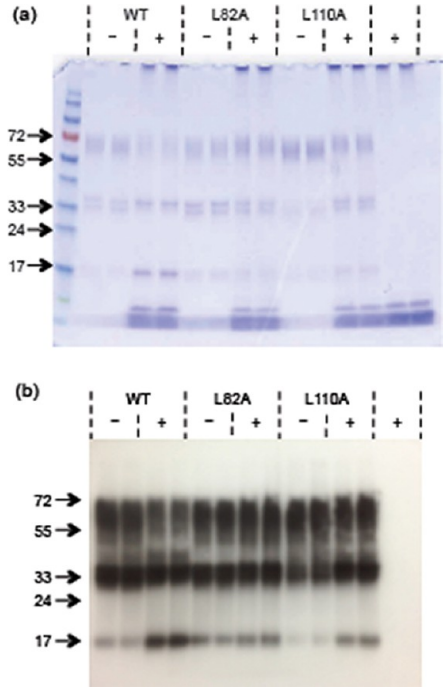

Figure 11. Cross-linking of TTR (wt and mutants) incubated without (−) and with (+) Aβ. Molecular mass markers are shown in the first lane. (a) Stained with Coomassie Blue. (b) Western blot with the anti-TTR antibody.

TTR in the absence of Aβ, we observed tetramers and dimers. (The dimer−dimer contacts are relatively small in area, while the monomer−monomer contact is extensive. Thus, dimers are cross-linked readily, while not all tetramers are efficiently cross-linked; on the basis of preliminary experiments, we know that some protein that is tetrameric in solution will not be cross-linked under our conditions.) When Aβ was added to wt, the tetramer band became weaker, a stronger dimer band emerged, and a monomer band was apparent. This pattern is clear with both Coomassie and anti-TTR staining (Figure 11a,b). With L110A, there was also an increase in the magnitude of dimer and monomer bands in the presence of Aβ, although the change may be somewhat smaller than that observed for wt. In contrast to wt or L110A, there was no discernible destabilization for L82A caused by addition of Aβ. These data are consistent with the native gel data obtained in the absence of cross-linking.

DISCUSSION

TTR Inhibits the Toxicity of Aβ, as a Direct Result of Binding to Aβ Oligomers. TTR inhibits Aβ toxicity in an *in vitro* cell culture, as shown in this study as well as in several other reports.[57,20,21] Brouillette et al. demonstrated that TTR inhibits Aβ toxicity *in vivo* using an animal model of repeated

dx.doi.org/10.1021/bi4001613 | *Biochemistry* 2013, 52, 2849−2861

intrahippocampal injections of Aβ oligomers.[28] Here, we observed that TTR mutants L82A and L110A, which bind less Aβ than wt, were ineffective at inhibiting toxicity. These results provide strong evidence of a direct cause-and-effect connection between TTR−Aβ binding and TTR-mediated protection against Aβ neurotoxicity.

With both wt and mTTR, complete recovery of cell viability was achieved at substoichiometric TTR:Aβ ratios; in fact, mTTR was somewhat more protective at equivalent mass concentrations than wt. The fact that complete protection is afforded at an ∼1:100 TTR:Aβ molar ratio suggests strongly that TTR is preferentially binding to toxic Aβ oligomers. To further test this hypothesis, we characterized Aβ aggregates over 7 days by both cross-linking (size) and immunoblotting (conformation). OC-positive aggregates, which can be either soluble or insoluble and are believed to have a fibrillar β-sheet structure,[22] were observed in all samples. Only low-molecular mass oligomers were present on day 0, and this sample bound poorly to TTR. Upon incubation for 1−5 days, some high-molecular mass (≳100 kDa) soluble Aβ aggregates appeared, and the level of binding of Aβ to TTR increased significantly. Longer (7 day) incubation led to the appearance of very large, insoluble aggregates, and the level of binding to TTR was again reduced. Thus, binding of Aβ to TTR correlates best with the presence of soluble Aβ aggregates containing roughly 25 to a few hundred monomers. These data strongly support our hypothesis that TTR binds selectively to soluble fibrillar Aβ oligomers, which are widely believed to be the most toxic form of Aβ. This hypothesis explains how TTR can fully protect against Aβ toxicity even when present at substoichiometric ratios (relative to Aβ monomers). We estimate an apparent equilibrium dissociation constant for TTR−Aβ binding of 10−100 nM from the toxicity data. It is not possible to define a true single equilibrium constant: the molar concentration of Aβ oligomers and the stoichiometry of TTR−Aβ binding are not known, there are two binding sites on TTR (EF helix and strand G), binding of Aβ to TTR to one binding site triggers exposure of the second binding site, and it is possible that different Aβ oligomeric species differ in their binding strengths.

TTR Suppresses Aβ Aggregate Growth, as a Direct Result of Binding. We introduce the use of nanoparticle tracking (NTA) to monitor Aβ aggregate growth. A particular advantage of this technique over DLS is that both aggregate size distribution and aggregate number concentration are quantified simultaneously. (DLS has an advantage in its sensitivity to smaller aggregates less than 50 nm in diameter.) Our results demonstrate clearly that Aβ aggregates grow in both number and size over time. The NTA data reveal that wt TTR suppresses Aβ aggregation in two ways: by preventing formation of new aggregates and by inhibiting growth of preexisting aggregates. However, preformed aggregates are not dissociated, nor does TTR cause a major restructuring of aggregates, because they are still OC-positive. We propose that TTR-mediated protection of cells from Aβ-induced neurotoxicity is accomplished by sequestering high-molecular mass soluble oligomers, coating them, and preventing their interaction with cells.

Both L110A and L82A slow but do not stop Aβ aggregate growth, and neither mutant is as effective as wt TTR in suppressing aggregation. With these data, the reduced level of binding of the mutants to Aβ is connected to their reduced efficacy at inhibiting aggregation. DLS experiments (conducted for 45 min) indicated L110A was somewhat more effective than L82A, while the longer (12 h) NTA experiments suggested L110A is somewhat less effective than L82A. Aβ binds to L110A at the EF helix/loop site (where L82 is) and to L82A at the interior site (strand G, where L110 is). The DLS and NTA data combined could be explained as follows. Binding of Aβ to the exposed L82 site (present in L110A) is faster, but ultimately thermodynamically weaker and less effective, while binding of Aβ to the interior L110 site (present in L82A) is slower because of greater steric restriction, but stronger and more effective for the suppression of growth.

Aβ Binding Induces Destabilization of TTR Quaternary Structure. We observed, by circular dichroism, a change in the wt TTR secondary structure upon its incubation with excess Aβ for 2 days; this change was absent with short incubation or if Aβ was incubated with L82A and L110A. TTR tetramers are remarkably stable, but it is well established that tetramers undergo slow monomer subunit exchange with a time constant of approximately 18−24 h.[27] The change in wt TTR secondary structure caused by Aβ was very similar to the difference in secondary structure between wt TTR and TTR mutants that are unstable tetramers (e.g., S85A), dimers (S112I), or monomers (F87M/L110M). We therefore hypothesize that Aβ induces destabilization of TTR tetramers. We obtained direct support for this hypothesis from both native gel electrophoresis and cross-linking experiments, demonstrating that wt TTR tetramers partially dissociate after incubation with Aβ for 1−2 days.

L82A tetramers were not destabilized when incubated with Aβ. From high-temperature experiments, we determined that the monomer exchange rates for L82A and wt are equal, so the lack of tetramer dissociation of L82A cannot be explained by differences in tetramer stability. Further experiments established that tetramer destabilization is not simply due to a detergent-like action of Aβ, because incubation of TTR with a detergent for 1−2 days caused partial dissociation of all three TTR variants equally. Finally, our data show that the slow kinetics of Aβ-induced TTR dissociation is not due to time-dependent changes in Aβ aggregates. On the basis of these combined results, we propose that binding of Aβ to the L82 site on TTR triggers tetramer destabilization and dissociation to monomers and/or dimers.

We have previously shown that monomeric and dimeric TTR mutants bind more Aβ than tetramers.[14] Furthermore, TTR that is chemically cross-linked to stabilized tetramers will bind less Aβ than un-cross-linked TTR (unpublished results). Thus, by destabilizing tetramers, binding of Aβ to L82 has the fortuitous effect of exposing the interior hydrophobic β-sheet (including L110), a potent binding site for Aβ.

Previously, we showed that Aβ can compete to some extent with reassociation of acid-dissociated TTR.[14] Thus, it is possible that the observed tetramer destabilization is due to binding of Aβ to TTR monomers during subunit exchange (in particular to the interior hydrophobic β-sheet) that competes with reassociation of the monomer to tetramers. L110A contains the L82 binding site and is destabilized by Aβ; this dissociation is likely further facilitated by its modestly higher tetramer instability (as measured by k_d). Aβ does not bind to the exposed interior β-sheet in L110A, but this mutant still is destabilized. Together with the lack of dissociation of L82A, this suggests that TTR destabilization is not strictly attributable to binding of Aβ to the hydrophobic interior β-sheet of dissociated TTR subunits and subsequent competition with TTR reassociation. However, this competitive binding could be

an additional mechanism that maintains wt TTR in the dissociated form.

TTR Is both a Sensor and a Scavenger of Toxic Aβ Oligomers. Our hypothesis can be stated briefly: The EF loop of TTR is the sensor, and the inner β-sheet is the scavenger, for Aβ oligomers. TTR must be tetrameric to conduct its normal functions as a transporter of thyroxine and retinol-binding protein. Furthermore, TTR monomers are prone to self-aggregation and amyloid formation.[29] There are several known natural TTR mutants that destabilize TTR tetramers; these mutations lead to aggregation and amyloid deposition and are associated with diseases such as familial amyloid polyneuropathy.[30,31] Thus, normally stable TTR tetramers are preferable, but TTR monomers bind more Aβ,[14] presumably because of greater solvent exposure of the hydrophobic inner β-sheet. In our proposed scenario, then, TTR remains safely tetrameric unless and until it detects unwanted Aβ oligomers. Exposure of the interior binding site is triggered when, and only when, the exterior loop of TTR senses the presence of Aβ oligomers.

This hypothesis is supported indirectly by our discovery of S85A, a TTR alanine mutant in which the mutation is in the EF loop. This mutant folds into less stable tetramers, binds more Aβ than wt,[13] and protects against Aβ toxicity in vitro (unpublished data). Similarly, the F87M mutation on the EF loop produced a mixture of tetramers and monomers.[16] Others have shown that low pH (3.5−4) causes conformational changes in the EF helix and loop that destabilize the tetramer; this is believed to be the first step in the TTR amyloidogenic pathway.[32] Together, these data support the hypothesis that changes in the EF helix/loop can destabilize tetramers. Initial binding between Aβ and TTR could be mediated through the EF helix/loop, triggering a conformational change that makes TTR more amyloidogenic, and thus more able to interact with Aβ. Furthermore, we previously showed that a monomeric TTR mutant (F87M/L110M) is more effective than TTR tetramers at arresting Aβ aggregate growth.[14] Thus, Aβ-mediated destabilization of tetramers leads to ever stronger TTR−Aβ association. While normally destabilized TTR is undesirable, in this case this is a favorable outcome, because the interaction between TTR and Aβ prevents Aβ toxicity.

Comparison of TTR to Synthetic Aβ Sequence-Derived Inhibitors. We and others have reported that short sequences derived from full-length Aβ can act as "recognition elements", binding to and disrupting normal Aβ aggregation pathways.[33−37] In our most effective compounds, we linked the recognition element KLVFF (residues 16−20 of Aβ) to a hexamer of charged polar amino acids or derivatives. Full protection against Aβ toxicity was obtained with a 10-fold excess of Aβ and partial protection with a 100-fold excess of Aβ (250 nM inhibitor to 25 μM Aβ).[38] In the work reported here, we observed that TTR afforded complete protection with a 100-fold excess of Aβ and partial protection with a 1000-fold excess of Aβ [∼20 nM or ∼1 μg/mL (Figure 2)]. Thus, TTR is 10-fold more protective than our best synthesized compounds. (However, it must be recognized that different cell lines were used to assess toxicity.)

For the Aβ sequence-derived compounds, our previous data were consistent with a mechanism by which the compounds inhibited toxicity by accelerating the growth of large aggregates. We hypothesized that the compounds reversibly associated with β-amyloid aggregates and, through effects on local solvent properties, enhanced hydrophobic interactions to drive association of smaller Aβ aggregates into larger, less toxic aggregates.[39,40] Such a mechanism would reduce the level of exposure of cells to smaller soluble oligomers that are more hydrophobic and presumably more toxic. TTR appears to act differently, because it arrests Aβ aggregation. We hypothesize that hydrophobic sites of TTR (particularly the inner β-sheet) bind tightly to exposed hydrophobic patches on Aβ oligomers, preventing both further Aβ−Aβ association and unwanted Aβ−cell association.

Relationship between TTR and AD. As described earlier, in transgenic mice engineered to express APP and develop amyloid deposits, TTR is upregulated; an increased level of synthesis of TTR may protect these mice from the neuronal death of full-blown AD.[1,2] Although normally CSF TTR is synthesized in the choroid plexus, a recent investigation demonstrated TTR synthesis in choroid plexus-free cortical cultures established from these transgenic mice, whereas minimal TTR synthesis was observed in wt controls.[5] Another study showed that APPsα mediates TTR expression.[41] These data suggest that APP and/or its proteolytic products trigger TTR synthesis, at least in transgenic mice.

In humans, plasma TTR levels fall in middle age or under conditions of malnutrition or chronic inflammation.[11] A statistically significant decrease in TTR plasma levels was observed in AD patients relative to age-matched controls, and among a cohort of AD sufferers, TTR levels were lower in those with more rapid cognitive decline.[42] These data, although very limited, hint that the decrease in TTR levels with age or disease could reduce TTR's normally protective role in sensing and scavenging toxic Aβ soluble oligomers. Perhaps restoring or replacing TTR's natural protective role would provide a safe therapeutic approach to treating AD.

AUTHOR INFORMATION

Corresponding Author

*Department of Chemical and Biological Engineering, 1415 Engineering Dr., Madison, WI 53706. E-mail: regina@engr.wisc.edu. Phone: (608) 262-1587.

Funding

Supported by National Institutes of Health Grant 2R01AG033493.

Notes

The authors declare no competing financial interest.

ABBREVIATIONS

Aβ, β-amyloid; AD, Alzheimer's disease; APP, amyloid precursor protein; CD, circular dichroism; CSF, cerebrospinal fluid; DLS, dynamic light scattering; DIV, days *in vitro*; MTS, 3-(4,5-dimethylthiazol-2-yl)-5-(3-carboxymethoxyphenyl)-2-(4-sulfophenyl)-2*H*-tetrazolium salt; NBM, neurobasal medium; NTA, nanoparticle tracking analysis; PMS, phenazine methosulfate; PBS, phosphate-buffered saline; PICUP, photoinduced cross-linking of unmodified proteins; PS, penicillin/streptomycin; RBP, retinol-binding protein; TBS, Tris-buffered saline; TTR, transthyretin; TUNEL, terminal deoxynucleotidyltransferase-mediated dUTP nick end labeling; wt, wild type.

REFERENCES

(1) Johnson, J. A., and Stein, T. D. (2002) Lack of neurodegeneration in transgenic mice overexpressing mutant amyloid precursor protein is associated with increased levels of transthyretin and the activation of cell survival pathways. *J. Neurosci. 22*, 7380−7388.

(2) Johnson, J. A., Stein, T. D., Anders, N. J., DeCarli, C., Chan, S. L., and Mattson, M. P. (2004) Neutralization of transthyretin reverses the

neuroprotective effects of secreted amyloid precursor protein (APP) in APP(Sw) mice resulting in tau phosphorylation and loss of hippocampal neurons: Support for the amyloid hypothesis. *J. Neurosci. 24*, 7707−7717.
(3) Shen, C. K. J., Tsai, K. J., Yang, C. H., Lee, P. C., Wang, W. T., and Chiu, M. J. (2009) Asymmetric expression patterns of brain transthyretin in normal mice and a transgenic mouse model of Alzheimer's disease. *Neuroscience 159*, 638−646.
(4) Wu, Z. L., Ciallella, J. R., Flood, D. G., O'Kane, T. M., Bozyczko-Coyne, D., and Savage, M. J. (2006) Comparative analysis of cortical gene expression in mouse models of Alzheimer's disease. *Neurobiol. Aging 27*, 377−386.
(5) Li, X. Y., Masliah, E., Reixach, N., and Buxbaum, J. N. (2011) Neuronal Production of Transthyretin in Human and Murine Alzheimer's Disease: Is It Protective? *J. Neurosci. 31*, 12483−12490.
(6) Liu, L., Hou, J., Du, J. L., Chumanov, R. S., Xu, Q. G., Ge, Y., Johnson, J. A., and Murphy, R. M. (2009) Differential modification of Cys10 alters transthyretin's effect on β-amyloid aggregation and toxicity. *Protein Eng., Des. Sel. 22*, 479−488.
(7) Giunta, S., Valli, M. B., Galeazzi, R., Fattoretti, P., Corder, E. H., and Galeazzi, L. (2005) Transthyretin inhibition of amylold β aggregation and toxicity. *Clin. Biochem. 38*, 1112−1119.
(8) Costa, R., Ferreira-da-Silva, F., Saraiva, M. J., and Cardoso, I. (2008) Transthyretin protects against A-β peptide toxicity by proteolytic cleavage of the peptide: A mechanism sensitive to the Kunitz Protease Inhibitor. *PLoS One 3*, No. e2899.
(9) Buxbaum, J. N., Ye, Z., Reixach, N., Friske, L., Levy, C., Das, P., Golde, T., Masliah, E., Roberts, A. R., and Bartfai, T. (2008) Transthyretin protects Alzheimer's mice from the behavioral and biochemical effects of Aβ toxicity. *Proc. Natl. Acad. Sci. U.S.A. 105*, 2681−2686.
(10) Potter, H., Costa, D. A., Craechiolo, J. R., Bachstetter, A. D., Hughes, T. F., Bales, K. R., Paul, S. M., Mervis, R. F., and Arendash, G. W. (2007) Enrichment improves cognition in AD mice by amyloid-related and unrelated mechanisms. *Neurobiol. Aging 28*, 831−844.
(11) Hamilton, J. A., and Benson, M. D. (2001) Transthyretin: A review from a structural perspective. *Cell. Mol. Life Sci. 58*, 1491−1521.
(12) Richardson, S. J. (2007) Cell and molecular biology of transthyretin and thyroid hormones. *Int. Rev. Cytol. 258*, 137−193.
(13) Du, J. L., Cho, P. Y., Yang, D. T., and Murphy, R. M. (2012) Identification of β-amyloid-binding sites on transthyretin. *Protein Eng., Des. Sel. 25*, 337−345.
(14) Du, J. L., and Murphy, R. M. (2010) Characterization of the interaction of β-amyloid with transthyretin monomers and tetramers. *Biochemistry 49*, 8276−8289.
(15) Schwarzman, A. L., Gregori, L., Vitek, M. P., Lyubski, S., Strittmatter, W. J., Enghilde, J. J., Bhasin, R., Silverman, J., Weisgraber, K. H., Coyle, P. K., Zagorski, M. G., Talafous, J., Eisenberg, M., Saunders, A. M., Roses, A. D., and Goldgaber, D. (1994) Transthyretin sequesters amyloid-β protein and prevents amyloid formation. *Proc. Natl. Acad. Sci. U.S.A. 91*, 8368−8372.
(16) Jiang, X., Smith, C. S., Petrassi, H. M., Hammarstrom, P., White, J. T., Sacchettini, J. C., and Kelly, J. W. (2001) An engineered transthyretin monomer that is nonamyloidogenic, unless it is partially denatured. *Biochemistry 40*, 11442−11452.
(17) Pallitto, M. M., and Murphy, R. M. (2001) A mathematical model of the kinetics of β-amyloid fibril growth from the denatured state. *Biophys. J. 81*, 1805−1822.
(18) Fancy, D. A., and Kodadek, T. (1999) Chemistry for the analysis of protein-protein interactions: Rapid and efficient cross-linking triggered by long wavelength light. *Proc. Natl. Acad. Sci. U.S.A. 96*, 6020−6024.
(19) Xia, K., Zhang, S. J., Bathrick, B., Liu, S. Q., Garcia, Y., and Colon, W. (2012) Quantifying the kinetic stability of hyperstable proteins via time-dependent SDS trapping. *Biochemistry 51*, 100−107.
(20) Murphy, R. M., Liu, L., Hou, J., Du, J. L., Chumanov, R. S., Xu, Q. G., Ge, Y., and Johnson, J. A. (2009) Differential modification of Cys10 alters transthyretin's effect on β-amyloid aggregation and toxicity. *Protein Eng., Des. Sel. 22*, 479−488.
(21) Costa, R., Goncalves, A., Saralva, M. J., and Cardoso, I. (2008) Transthyretin binding to A-β peptide: Impact on A-β fibrillogenesis and toxicity. *FEBS Lett. 582*, 936−942.
(22) Glabe, C. G. (2008) Structural classification of toxic amyloid oligomers. *J. Biol. Chem. 283*, 29639−29643.
(23) Filipe, V., Hawe, A., and Jiskoot, W. (2010) Critical Evaluation of Nanoparticle Tracking Analysis (NTA) by NanoSight for the Measurement of Nanoparticles and Protein Aggregates. *Pharm. Res. 27*, 796−810.
(24) Glabe, C. G., Kayed, R., Head, E., Sarsoza, F., Saing, T., Cotman, C. W., Necula, M., Margol, L., Wu, J., Breydo, L., Thompson, J. L., Rasool, S., Gurlo, T., and Butler, P. (2007) Fibril specific, conformation dependent antibodies recognize a generic epitope common to amyloid fibrils and fibrillar oligomers that is absent in prefibrillar oligomers. *Mol. Neurodegener. 2*, 18.
(25) Sarsoza, F., Saing, T., Kayed, R., Dahlin, R., Dick, M., Broadwater-Hollifield, C., Mobley, S., Lott, I., Doran, E., Gillen, D., Anderson-Bergman, C., Cribbs, D. H., Glabe, C., and Head, E. (2009) A fibril-specific, conformation-dependent antibody recognizes a subset of Aβ plaques in Alzheimer disease, Down syndrome and Tg2576 transgenic mouse brain. *Acta Neuropathol. 118*, 505−517.
(26) Glabe, C. G., Kayed, R., Head, E., Thompson, J. L., McIntire, T. M., Milton, S. C., and Cotman, C. W. (2003) Common structure of soluble amyloid oligomers implies common mechanism of pathogenesis. *Science 300*, 486−489.
(27) Keetch, C. A., Bromley, E. H. C., McCammon, M. G., Wang, N., Christodoulou, J., and Robinson, C. V. (2005) L55P transthyretin accelerates subunit exchange and leads to rapid formation of hybrid tetramers. *J. Biol. Chem. 280*, 41667−41674.
(28) Brouillette, J., Caillierez, R., Zommer, N., Alves-Pires, C., Benilova, I., Blum, D., De Strooper, B., and Buee, L. (2012) Neurotoxicity and Memory Deficits Induced by Soluble Low-Molecular-Weight Amyloid-β(1−42) Oligomers Are Revealed In Vivo by Using a Novel Animal Model. *J. Neurosci. 32*, 7852−7861.
(29) Hammarstrom, P., Sekijima, Y., White, J. T., Wiseman, R. L., Lim, A., Costello, C. E., Altland, K., Garzuly, F., Budka, H., and Kelly, J. W. (2003) D18G transthyretin is monomeric, aggregation prone, and not detectable in plasma and cerebrospinal fluid: A prescription for central nervous system amyloidosis? *Biochemistry 42*, 6656−6663.
(30) McCutchen, S. L., Colon, W., and Kelly, J. W. (1993) Transthyretin mutation Leu-55-Pro significantly alters tetramer stability and increases amyloidogenicity. *Biochemistry 32*, 12119−12127.
(31) Babbes, A. R. H., Powers, E. T., and Kelly, J. W. (2008) Quantification of the thermodynamically linked quaternary and tertiary structural stabilities of transthyretin and its disease-associated variants: The relationship between stability and amyloidosis. *Biochemistry 47*, 6969−6984.
(32) Palaninathan, S. K., Mohamedmohaideen, N. N., Snee, W. C., Kelly, J. W., and Sacchettini, J. C. (2008) Structural Insight into pH-induced Conformational Changes within the Native Human Transthyretin Tetramer. *J. Mol. Biol. 382*, 1157−1167.
(33) Ghanta, J., Shen, C. L., Kiessling, L. L., and Murphy, R. M. (1996) A strategy for designing inhibitors of β-amyloid toxicity. *J. Biol. Chem. 271*, 29525−29528.
(34) Findeis, M. A., Musso, G. M., Arico-Muendel, C. C., Benjamin, H. W., Hundal, A. M., Lee, J. J., Chin, J., Kelley, M., Wakefield, J., Hayward, N. J., and Molineaux, S. M. (1999) Modified-peptide inhibitors of amyloid β-peptide polymerization. *Biochemistry 38*, 6791−6800.
(35) Tjernberg, L. O., Naslund, J., Lindqvist, F., Johansson, J., Karlstrom, A. R., Thyberg, J., Terenius, L., and Nordstedt, C. (1996) Arrest of β-amyloid fibril formation by a pentapeptide ligand. *J. Biol. Chem. 271*, 8545−8548.
(36) Gordon, D. J., Sciarretta, K. L., and Meredith, S. C. (2001) Inhibition of β-amyloid(40) fibrillogenesis and disassembly of β-amyloid(40) fibrils by short β-amyloid congeners containing N-methyl amino acids at alternate residues. *Biochemistry 40*, 8237−8245.

(37) Rangachari, V., Davey, Z. S., Healy, B., Moore, B. D., Sonoda, L. K., Cusack, B., Maharvi, G. M., Fauq, A. H., and Rosenberry, T. L. (2009) Rationally designed dehydroalanine (ΔAla)-containing peptides inhibit amyloid-β (Aβ) peptide aggregation. *Biopolymers 91*, 456−465.
(38) Lowe, T. L., Strzelec, A., Kiessling, L. L., and Murphy, R. M. (2001) Structure-function relationships for inhibitors of β-amyloid toxicity containing the recognition sequence KLVFF. *Biochemistry 40*, 7882−7889.
(39) Kim, J. R., Gibson, T. J., and Murphy, R. M. (2003) Targeted control of kinetics of β-amyloid self-association by surface tension-modifying peptides. *J. Biol. Chem. 278*, 40730−40735.
(40) Kim, J. R., and Murphy, R. M. (2004) Mechanism of accelerated assembly of β-amyloid filaments into fibrils by KLVFFK6. *Biophys. J. 86*, 3194−3203.
(41) Li, H. M., Wang, B. P., Wang, Z. L., Guo, Q. X., Tabuchi, K., Hammer, R. E., Sudhof, T. C., and Zheng, H. (2010) Soluble amyloid precursor protein (APP) regulates transthyretin and Klotho gene expression without rescuing the essential function of APP. *Proc. Natl. Acad. Sci. U.S.A. 107*, 17362−17367.
(42) Velayudhan, L., Killick, R., Hye, A., Kinsey, A., Guentert, A., Lynham, S., Ward, M., Leung, R., Lourdusamy, A., To, A. W. M., Powell, J., and Lovestone, S. (2012) Plasma transthyretin as a candidate marker for Alzheimer's disease. *J. Alzheimer's Dis. 28*, 369−375.